WILEY-VCH

Yi Zhang, Hui Dong, Hans-Joachim Krause,
Guofeng Zhang, and Xiaoming Xie

SQUID Readout Electronics and Magnetometric Systems for Practical Applications

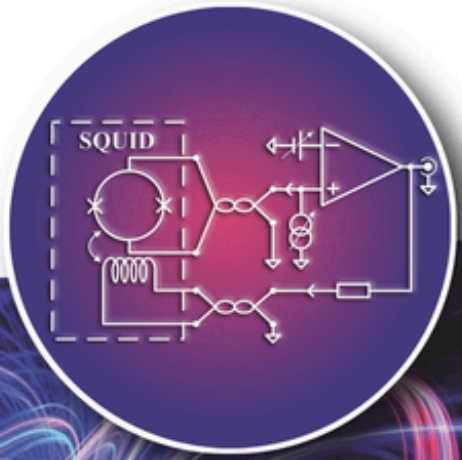

SQUID Readout Electronics and Magnetometric Systems for Practical Applications

SQUID Readout Electronics and Magnetometric Systems for Practical Applications

Yi Zhang
Hui Dong
Hans-Joachim Krause
Guofeng Zhang
Xiaoming Xie

WILEY-VCH

Authors

Prof. Dr. Yi Zhang
Forschungszentrum Jüelich (Retired)
Institute of Biological Information Processing
Wilhelm-Johnen-Straße
52428 Jüelich
Germany

Prof. Dr. Hui Dong
Shanghai Institute of Microsystem and Information Technology
865 Changning Road
200050 Shanghai
China

Prof. Dr. Hans-Joachim Krause
Forschungszentrum Jüelich
Institute of Biological Information Processing
Wilhelm-Johnen-Straße
52428 Jüelich
Germany

Dr. Guofeng Zhang
Shanghai Institute of Microsystem and Information Technology
865 Changning Road
200050 Shanghai
China

Prof. Dr. Xiaoming Xie
Shanghai Institute of Microsystem and Information Technology
ShanghaiTech University
University of Chinese Academy of Sciences
865 Changning Road
200050 Shanghai
China

Library of Congress Card No.: applied for

British Library Cataloguing-in-Publication Data
A catalogue record for this book is available from the British Library.

Bibliographic information published by the Deutsche Nationalbibliothek
The Deutsche Nationalbibliothek lists this publication in the Deutsche Nationalbibliografie; detailed bibliographic data are available on the Internet at <http://dnb.d-nb.de>.

Print ISBN: 978-3-527-34488-8
ePDF ISBN: 978-3-527-81650-7
ePub ISBN: 978-3-527-81652-1
oBook ISBN: 978-3-527-81651-4

Cover Design Adam-Design, Weinheim, Germany
Typesetting SPi Global, Chennai, India
Printing and Binding

Printed on acid-free paper

10 9 8 7 6 5 4 3 2 1

Contents

Preface

Time flies! Thirteen years ago, as a research professor at Shanghai Institute of Microsystem and Information Technology (SIMIT), Chinese Academy of Sciences (known as Shanghai Institute of Metallurgy by that time), I was charged with a challenging mission, to start a team on superconducting electronics research. From the institute, it was a quite straightforward decision, as the whole institute had been gradually shifting from materials science research toward electronics and systems. And for myself, it was not so easy to start something new at the age over 40, with a strong background on superconducting materials, some basic knowledge on electronics but little on superconducting electronics. Just when I was wondering how to do that, Prof. P.H. Wu, a member of Chinese Academy of Sciences, a famous professor in the field of superconducting electronics in China, who had worked at Research Center Julich (FZJ) Germany, recommended me Dr. Yi Zhang, a reputable German scientist at FZJ, born in Shanghai, acknowledged globally for his excellent research on the development of high T_c radio-frequency superconducting quantum interference devices (high temperature superconducting [HTS] rf SQUIDs), their readout electronics and systems. I contacted FZJ without hesitation, inviting Yi to act as a consultant to our first project on SQUID-based Magnetocardiography (MCG) system. This request letter opened the door of cooperation between SIMIT and FZJ. To date, our cooperation has developed from a project collaboration between two professors to the establishment of two joint research laboratories and further to a virtual joint research institute. The cooperation also has been extended from superconductivity to topological insulators and quantum computing.

After some formal procedures, I got the approval of my request letter from Prof. Dr. Joachim Treusch, the former chairman of the board of directors of FZJ, Prof. Dr. Sebastian Schmidt, a current member of the board of directors of FZJ, and Prof. Dr. Andreas Offenhäusser, director of IBN2 (Institute of Bio and Nanoscience, now Institute of Biological Information Processing), which Yi belonged to. Besides the support from the top management, the involvement of Prof. Dr. Hans-Joachim Krause, team leader of magnetic sensors in IBN2, was another important step for our successful cooperation.

Our joint research on dc SQUID started from the development of asymmetrical SQUID characteristics, in an attempt to simply SQUID readout and system

design. The adventure was full of excitement and frustration. Early in the morning, we sat together, planning the work of the day, late in the evening, we summarized our results from the notes we made during the day, sometimes exciting progress, sometimes frustrating results, and sometimes confusing results which we could not describe easily. I still remember how excited we were when we first observed the asymmetrical flux-current characteristics of a SQUID on the oscilloscope, and I remembered as well how much we were frustrated when we learnt that the desired asymmetrical characteristics did not lead to the lower noise we had sought for so long. The notes piled up day after day, getting thicker and thicker, we called them "Rabe's Diary." After numerous discussions back and forth, we succeeded in interpreting our results, which led to our first joint publication and our joint patent on the so-called "SQUID Bootstrap Circuit," and to many other joint publications in the following 10 more years.

The SQUID research was more difficult than we first thought because setting up SQUID systems for applications requires the involvement of people from several different disciplines. A complete understanding for SQUID systems needs comprehensive knowledge not only in quantum physics and low-temperature physics but also in material science and electronics engineering. In fact, electrical or electronics engineers are always needed for system development. Therefore, it is very important to establish a common language that is easily accessible for all people. That was how we got the idea to write this book.

Yi Zhang contributed most to writing of this book, with his experience in SQUID research for 34 years, including more than 10 years of joint research with SIMIT. We have aimed to write this book in a way that is easily understandable for engineers and students, in order to overcome the formidable barrier of "quantum" physics. In this book, e.g. dc SQUIDs are simply treated as resistor-like elements, which are modulated by the magnetic flux. We hope that this book will be appreciated by all people interested in developing and working with SQUIDs and SQUID systems. By inviting engineers into the SQUID "family," we will have a better chance to transform SQUID from a laboratory toy to an enabling technology that will eventually shape our life.

This book is largely a documentation of the joint achievements accomplished in the cooperation between SIMIT and FZJ in the field of superconducting electronics. We believe that the ongoing collaboration between the two parties will continue to grow, and the cooperation will bring more achievements not only in the field of superconducting electronics but also in other fields in the future.

November 2019.

Xiaoming Xie
Shanghai, China

Acknowledgments

It is our pleasure to acknowledge the generous assistance that has been offered throughout the preparation of this book. Without such help, our task would not have been possible. We owe a special debt of gratitude to all the colleagues from China and Germany who have contributed to the works mentioned in this book. Special thanks to Dr. M. Mück for your constructive comments on Chapter 6. Very special thanks to Dr. H. Soltner for the English language reading. We finally express our heartfelt gratitude to Wiley.

1

Introduction

1.1 Motivation

Superconducting QUantum Interference Devices (SQUIDs) are well known because they are the most sensitive sensors for measuring magnetic flux. In magnetometry, a SQUID with a field-to-flux transformer circuit (converter) construct is a magnetometer with high field sensitivity in the range of $\mathrm{fT}/\sqrt{\mathrm{Hz}}$ (one millionth of the earth's magnetic field). Therefore, the study of SQUID systems has never stopped.

Many books and reviews have elaborated on the SQUID principle and SQUID magnetometric systems as well as SQUID applications, e.g. "Superconductor Applications: SQUIDs and Machines" edited by B. B. Schwartz and S. Foner [1], "Physics and Applications of the Josephson Effect" edited by A. Barone and G. Paterno [2], and the NATO proceedings "SQUID Sensors: Fundamentals, Fabrication and Applications" edited by H. Weinstock [3]. In particular, "The SQUID Handbook," edited in 2004 by John Clarke and Alex I. Braginski comprehensively summarizes SQUID's theory and practice since SQUIDs have been discovered [4]. Hence, this book has become the new "bible" for researchers in the field. Furthermore, the review of "SQUID Magnetometers for Low-Frequency Applications" by Tapani Ryhänen et al. presented a novel formulation for SQUID operation and SQUID magnetometers for low-frequency applications, taking into account the coupling circuits and electronics [5].

Structurally, a direct current (dc) SQUID is a superconducting ring interrupted with two Josephson junctions. Predicatively, SQUIDs have very rich physical meanings, e.g. the Aharonov–Bohm effect, flux quantization, Meissner effect, Bardeen–Cooper–Schrieffer (BCS) theory, and the Josephson tunnel effect. However, starting from the view of electronic circuits, our first question is on what a dc SQUID is. In magnetometry, a dc SQUID should be regarded as a resistor-like element where its dynamic resistance is modulated by the flux Φ threading the SQUID's loop. In the readout technique, the dynamic resistance of the SQUID, $R_{\mathrm{d}}(\Phi) = \partial V/\partial I$, i.e. the derivative of the voltage with respect to current, is the fundamental readout quantity, which is embodied in the current–voltage (I–V) characteristics of the SQUID. Here, the changing I–V characteristics are limited by two curves at the integer (upper limit) and half-integer (lower limit) of the flux quantum Φ_0, which reflect the quantity

SQUID Readout Electronics and Magnetometric Systems for Practical Applications,
First Edition. Yi Zhang, Hui Dong, Hans-Joachim Krause, Guofeng Zhang, and Xiaoming Xie.

of magnetic flux in the SQUID loop. There is already abundant "know-how" to read out a resistor R. For example, one can measure a voltage V across R with a constant current flowing through R or measure a current I through R when a constant voltage V is connected to R in parallel. A dc SQUID can either be operated at constant current by measuring the voltage across it (called current bias mode) or at constant voltage by measuring the current through it (called voltage bias mode). In either bias mode, only the SQUID's $V(\Phi)$ or $I(\Phi)$ characteristics emerge. Similar to the change in I–V characteristics with the flux, $V(\Phi)$ and $I(\Phi)$ are also modulated by Φ. In brief, the essence of all three SQUID characteristics is recording the SQUID's dynamic resistance changes, $R_d(\Phi)$.

Generally, a SQUID system consists of the SQUID sensor and its readout electronics. The small SQUID signal leads to difficulty in reading out the SQUID's signal without additional noise contributions from the readout technique. Conventionally, one hopes to suppress such noise contribution below the intrinsic SQUID noise $\delta\Phi_s$. In other words, the measured system noise almost reaches $\delta\Phi_s$.

The main noise source in readout electronics is the preamplifier, which possesses two independent noise sources: the voltage noise V_n and the current noise I_n. Both of these noise sources are innate to the amplifier chip and cannot be changed. In order to compare these two noise contributions in a SQUID system, both types of electronic noise should be translated into a flux noise, $\delta\Phi_e$, in units of $\Phi_0/\sqrt{\text{Hz}}$ with SQUID's transfer coefficient of $\partial V/\partial\Phi$ or $\partial I/\partial\Phi$. In fact, the original SQUID parameters including the transfer coefficients are also innate to the particular SQUID and cannot be changed. However, the SQUID's apparent parameters at the input terminal of the preamplifier can be modified. Over the past half century, people have developed different readout schemes, where the electronic noise $\delta\Phi_e$ is suppressed by increasing the apparent transfer coefficients once a preamplifier is selected. Indeed, the modification of the apparent parameters is the main thread running through the book. Here, we will change the perspective to discuss the optimization of the SQUID system noise, i.e. how to match the SQUID parameters with the readout electronics.

According to the type of superconducting material used, SQUIDs can be divided into two groups: the low-temperature superconducting (LTS) SQUID, also called low-T_c SQUID, usually operated at 4.2 K (liquid helium temperature); and the high-temperature superconducting (HTS) SQUID, also called high-T_c SQUID, usually operated at 77 K (the liquid nitrogen temperature). The LTS material is typically niobium and HTS material is yttrium barium copper oxide ($YB_2Cu_3O_{7-x}$).

However, according to the working principles, the dc SQUID mentioned above is completely different from the radio frequency (rf) SQUID, which is a superconducting ring interrupted with only one junction. To read the signal from an rf SQUID, it is inductively coupled to an rf tank circuit, which connects to the readout electronics.

In this book, LTS (low-T_c) dc SQUID and HTS (high-T_c) rf SQUID systems, which are often used in magnetometry, will be highlighted. We will share our experiences and lessons, mostly from our own works, with readers, college students, and graduates in physics and engineering who have an interest in SQUID techniques, e.g. how to set up a simple SQUID system for themselves.

1.2 Contents of the Chapters

The book is organized into 12 chapters, where most of the content (from Chapters 2–11) is about the dc SQUIDs, and only the last chapter is related to rf SQUIDs. However, the dc SQUID bias reversal scheme [6], the $1/f$ noise study [7, 8], and the special readout scheme for the nano-SQUID [9, 10] are not included.

Chapter 1: This chapter is devoted to our motivation above and the subsequent chapter contents – why did we write this book, and what is it about?

Chapter 2: Because the Josephson junction (JJ) is the key element of SQUIDs, Josephson's equations should be first introduced. Then, JJs are analyzed with the resistively and capacitively shunted junction (RCSJ) model, thus introducing two important parameters: the Stewart–McCumber parameter β_c and the thermal rounding parameter Γ. To observe the features of JJs, one often uses the I–V characteristics, where the hysteresis behavior depends on the values of both β_c and Γ. Actually, the I–V characteristics describe the changing dynamic resistances R_d of the JJ, i.e. $R_d = \partial V/\partial I$. It was experimentally verified that the value of R_d depends not only on the junction shunt resistor R_j but also on the junction critical current I_c. Generally, JJs without hysteresis are suitable for SQUID operation. In fact, one habitually transforms the parameters β_c and Γ of the JJ into SQUID operation.

Chapter 3: For readout electronics, the dc SQUID is regarded as dynamic resistance $R_d(\Phi)$ modulated by the flux threading into the SQUID loop. The SQUID's I–V characteristics can be divided into three regions, and the SQUID is operated in the flux-modulated region (II). In fact, the behavior of $R_d(\Phi)$ is embodied in a SQUID's I–V characteristics. To measure a resistance R_d, one can impress a known current (current bias) into a SQUID and observe the voltage across the SQUID's dynamic resistance R_d. Alternatively, one can apply a constant voltage to the SQUID (voltage bias) and measure the current passing through R_d. Owing to the small $R_d \approx 10\,\Omega$ of the SQUID, an ideal current bias mode for SQUID operation can easily be realized. In contrast, an ideal voltage bias mode can hardly be achieved, as will be shown in the course of the chapter.

Chapter 4: Almost all SQUID readout electronics developed over the past half century have a common feature: they establish a so-called flux-locked loop (FLL) to realize linearization of the output voltage $V_{out}(\Phi)$ of the readout electronics; i.e. V_{out} is proportional to the flux change Φ. In this chapter, the principle and realization of the FLL are explained. It is a nulling method where a compensation flux always follows the measured flux, thus resulting in a total flux change of zero in the SQUID loop. In the FLL, the concept of the working point $\mathbb{W}$ comes up, and the "locked" and "unlocked" cases are discussed. In the FLL, a small flux change $\Delta\Phi$ near the working point $\mathbb{W}$ appears transiently, and a counter flux $-\Delta\Phi$ immediately compensates it so that the SQUID is continuously operated at a constant flux state. Therefore, the SQUID's $R_d(\Phi)$ near $\mathbb{W}$ can be expressed as $R_d(\Phi) = R_d + \Delta R_d$, where R_d is considered a fixed resistance and ΔR_d is a minor change with flux. According to the SQUID's bias modes, ΔR_d is translated into the readout quantity ΔV (or ΔI). For example, in practice, a current-biased SQUID can be regarded as a voltage source, $\Delta V = \Delta\Phi \times (\partial V/\partial\Phi)$, connecting to the fixed R_d in series (which seems to be the internal resistance

of the voltage source), where $(\partial V/\partial\Phi)$ is the SQUID's flux-to-voltage transfer coefficient at the working point W. The description of the SQUID by means of a differential dynamic resistance is a new model concept.

Chapter 5: In the case of a direct readout scheme (DRS) where the SQUID directly connects to a preamplifier, the electronics noise $\delta\Phi_e$ is usually much larger than the SQUID intrinsic noise $\delta\Phi_s$. Two types of preamplifiers, commercial op-amps (e.g. AD797 from Analog Devices Inc. or LT1028 from Linear Technology Corp.) and parallel-connected bipolar pair transistors (PCBTs) (e.g. $3\times$SSM2210 or $3\times$SSM2220 from Analog Devices Inc.), are the most commonly used. Here, the noise characteristics, V_n and I_n, of these two types of preamplifiers are measured separately. Nevertheless, a DRS exhibits several advantages; e.g. the SQUID's original parameters can be directly determined, and the noise contributions from both sides, $\delta\Phi_e$ and $\delta\Phi_s$, can be separately analyzed. Especially, the SQUID's transfer coefficient $\partial V/\partial\Phi$ $(\partial I/\partial\Phi)$ at the working point W plays two important roles: (i) it bridges different kinds of noise sources, thus unifying all noise in units of $\Phi_0/\sqrt{\text{Hz}}$, as the SQUID is a flux sensor; and (ii) a large transfer coefficient is beneficial for reducing $\delta\Phi_e$. In fact, it was experimentally confirmed that the noise contribution of $\delta\Phi_e$ does not depend on the SQUID's bias modes. Furthermore, for strongly damped SQUIDs, $\delta\Phi_e$ in DRS dominates the system noise $\delta\Phi_{sys}$.

Chapter 6: In a SQUID magnetometric system, one strives for a high magnetic field sensitivity δB_{sys}, which involves two aspects: a field-to-flux transformer circuit (converter) and an ordinary SQUID system with an FLL. The former converts a magnetic field signal B into a flux Φ threading the SQUID loop, while the latter reads out the picked-up Φ. In Section 6.1, the requirements of the converter are discussed. In Section 6.2, we show that the SQUID system is characterized by three dimensionless parameters, β_c, Γ, and β_L. Note that the definitions of β_c and Γ for only a single JJ are given in Chapter 2. During SQUID operation, both parameters must be given a new connotation. Four SQUIDs with different β_c values were characterized. Here, a reasonable interpretation of the observed absence of hysteresis in the SQUID's I–V characteristics at high β_c is given. For SQUID operation, the dimensionless parameter β_L particularly describes the modulation depth of the SQUID. Importantly, $\beta_L \approx 1$ imposes a design condition on the product $L_s I_c$ – namely, all electrically readable values of SQUID parameters increase with increase in the SQUID's nominal β_c.

Chapter 7: The flux modulation scheme (FMS) was first introduced to the SQUID readout in 1968 and quickly became the standard readout technique for current-biased SQUIDs. To date, FMS electronics have been the most extensively used. The basic idea of the FMS is to perform an up-conversion of the SQUID's voltage swing at the input terminal of the preamplifier with a step-up transformer, thus reducing the noise contribution of $\delta\Phi_e$. In contrast to a DRS, where a dc circuit (amplifier and integrator) is employed, the FMS is an ac circuit, e.g. operating in the 100 kHz frequency range, because the transformer can pass only ac signals. However, a SQUID is often used to detect magnetic flux signals Φ with slow changes, even quasi-static signals. To resolve this challenge, a high-frequency modulation of the SQUID signal is employed in order to transform the low-frequency magnetic flux signal into the high-frequency

regime. After up-conversion, demodulation is employed to convert the flux signal back to the low-frequency regime, thus realizing the transitions between ac and dc circuits.

If a SQUID is shunted by an element with impedance Z_s (e.g. the transformer), a change in the bias mode occurs. We introduce a dimensionless parameter $\chi = Z_s/R_d$ to quantitatively characterize the bias modes. In Section 7.1, we first introduce the so-called "mixed bias mode" concept. In Section 7.2, the FMS is discussed along with a conventional explanation. In Section 7.3, we revisit the FMS by analyzing the bias mode and the transfer characteristics of a step-up transformer.

Chapter 8: The DRS with flux feedback circuits in the "head stage" at the cryogenic temperature is highlighted in this chapter and in Chapter 9. The chapter starts with a comprehensive comparison of the different feedback schemes that have been employed in the recent decades. The techniques of additional positive feedback (APF), bias current feedback (BCF), and noise cancellation (NC) are categorized and discussed. Generally, there are two typical kinds of flux feedback circuits, the parallel feedback circuit (PFC) described in Chapter 8 and the series feedback circuit (SFC), which will follow in Chapter 9.

Indeed, we often use the differential chain rule of $R_d = (\partial V/\partial I) = (\partial V/\partial \Phi)/(\partial I/\partial \Phi)$ to analyze the flux feedback circuits. With the PFC, $(R_d)_{PFC}$ and $(\partial V/\partial \Phi)_{PFC}$ increase synchronously, while $(\partial I/\partial \Phi)_{PFC} = (\partial I/\partial \Phi)$ remains constant. However, using the SFC, $(R_d)_{SFC}$ decreases with the simultaneous increase in $(\partial I/\partial \Phi)_{SFC}$ because $(\partial V/\partial \Phi)_{SFC} = (\partial V/\partial \Phi)$. In fact, the large $(\partial V/\partial \Phi)_{PFC}$ has the benefit of suppressing the preamplifier's V_n. Separately, the large $(\partial I/\partial \Phi)_{SFC}$ reduces the noise contribution from the preamplifier's I_n. Although the behaviors of the apparent $V(\Phi)$ or $I(\Phi)$ in the two bias modes with the flux feedbacks (PFC and SFC) are very different, the effects of $\delta\Phi_e$ suppression are the same.

The PFC consists of a resistor R_p connected to a coil L_p in series that shunts to the SQUID, where L_p couples to the SQUID with a mutual inductance M_p. To simplify the analysis, we always take the flux feedback circuit in voltage bias mode, where two branches, the SQUID and PFC, are independent. Thus, the critical conditions of both flux feedbacks are easily obtained. In addition, we quantitatively analyze the PFC parameters and give their recommended regimes of operation. Indeed, it was experimentally proved that our analyses of both flux feedbacks agree well with the measured data.

Chapter 9: The SFC consists of a coil L_{se} connected to the SQUID in series, where L_{se} couples to the SQUID with a mutual inductance M_{se}. Because of SFC, the SQUID's apparent parameters $(R_d)_{SFC}$ at the input terminal of the preamplifier are reduced, thus reducing the preamplifier's current noise contribution, $\delta\Phi_{In}$.

A possible combination of the PFC and SFC is also discussed in Chapter 9. In practice, the two flux feedbacks via M_{se} and M_p are not independent, so adjusting M_{se} can also change M_p of the PFC, and vice versa. This leads to difficulties in reaching the designed mutual inductances. According to our experience, we do not recommend employing both flux feedbacks at the same time. For general SQUID applications, we suggest two practical concepts with flux feedback in a DRS: (i) an op-amp (preamplifier) with the PFC and (ii) a PCBT with the SFC.

Chapter 10: In many applications, the objective of a SQUID system is not to achieve utmost sensitivity but to rather have a SQUID system with simplicity, user-friendliness, robustness, with a high resistance against disturbances, good stability, and acceptable system noise $\delta\Phi_{sys}$. In this way, we should abandon the traditional ideas to pursue a low readout electronics noise $\delta\Phi_e$ that is lower than the intrinsic SQUID noise $\delta\Phi_s$. In contrast, tolerating a relatively large $\delta\Phi_s$ of a weakly damped SQUID with a large β_c to achieve a suitable $\delta\Phi_{sys}$ is a practical approach. Indeed, our novel paradigm for SQUID readout is to strive for equally high SQUID and electronics noise, $\delta\Phi_s \approx \delta\Phi_e$, as a basis to set up a simple and reliable SQUID system. The drawback of always striving for lowest SQUID system noise is the vulnerability of the system to fitting the exact amount of feedback in PFC or SFC schemes, thus leading to complexity and instability of the SQUID readout circuitry. Our concept of a weakly damped SQUID system does not yield the very best system noise $\delta\Phi_{sys}$ but rather a $\delta\Phi_{sys}$, which is suitable for applications. Most importantly, this concept tolerates deviations of the SQUID parameters in a large range, as we have shown by performing a statistical analysis of 101 SQUID magnetometers. Thereby, we proved the applicability of weakly damped SQUIDs with DRS to be employed in a multichannel SQUID system. For this purpose, "single-chip readout electronics" (SCREs) consisting of only one op-amp was developed. The equivalent circuit of the SCRE is used as the cover of this book. We characterized this system and demonstrated its applicability to magnetocardiography (MCG) and the transient electromagnetic (TEM) method in geophysical measurements.

Chapter 11: Two special dc SQUID readout schemes, the two-stage scheme and the double relaxation oscillation (D-ROS) scheme, are introduced. Both of them are suitable for observation of the SQUID's intrinsic noise $\delta\Phi_s$, i.e. $\delta\Phi_e < \delta\Phi_s$. In fact, the $\delta\Phi_s$ values in the two readout schemes are quite different. The two-stage readout scheme possesses a very small $\delta\Phi_e$, which can be lower than the $\delta\Phi_s$ of a SQUID with $\beta_c < 1$. In contrast, the un-shunted SQUID in the D-ROS scheme presents a large $\delta\Phi_s$ and a large $\partial V/\partial\Phi$, thus leading to $\delta\Phi_s < \delta\Phi_e$ in the system.

Actually, the two-stage readout scheme consists of a voltage-biased sensing SQUID and a sensitive SQUID-ammeter (the reading SQUID). The real trick of the two-stage scheme is the "flux amplifier," where the reading SQUID measures only the "amplified flux." In the closed voltage biased circuit of the sensing SQUID, a ring current $\Delta I = \Delta\Phi \times (\partial I/\partial\Phi)_{Sensing}$ is modulated by the measured flux $\Delta\Phi$. Here, ΔI flows through a coil L_a which is inductively coupled to the reading SQUID via the mutual inductance M_a, thus generating a further flux in the reading SQUID. Thus, the flux of $\Delta I \times M_a$ for the reading SQUID is amplified by a factor, $G_F = [(\partial I/\partial\Phi)_{Sensing} \times M_a]$, where $G_F > 1$. Therefore, the system noise of the reading SQUID can be regarded as the readout noise $\delta\Phi_e$ for the sensing SQUID. In other words, the two-stage scheme realizes a readout electronics noise $\delta\Phi_e$ below the product of $G_F \times (\delta\Phi_s)_{Sensing}$. In brief, for intrinsic SQUID noise studies, the $\delta\Phi_s$ of most SQUIDs is calibrated with the two-stage readout scheme.

The key elements of the D-ROS readout scheme are a hysteretic SQUID and a shunted circuit, the latter of which consists of a coil L_{ro} and a resistor R_{ro} in series. Here, the L_{ro} is not coupled to the SQUID. When a constant current I_b above the SQUID's I_c flows through the parallel circuit, the D-ROS becomes active

to oscillate. In fact, the initial motivation of the D-ROS readout scheme was to achieve a high flux-to-voltage transfer coefficient $\partial V/\partial\Phi$, e.g. in the $10\,\mathrm{mV}/\Phi_0$ region, thus simplifying the readout electronics and improving the slew rate. As an important consequence, the $\delta\Phi_s$ and the value of $\partial V/\partial\Phi$ in D-ROS scheme are high due to the un-shunted SQUID parameter $\beta_c \to \infty$. However, the system noise $\delta\Phi_{sys}$ of D-ROS is still acceptable for recording signals of, e.g. human biomagnetism; moreover, the large $\delta\Phi_s$ ($\approx\delta\Phi_{sys}$) improves the system robustness. Therefore, some commercial multichannel SQUID systems for MCG and magnetoencephalography (MEG) are equipped with the D-ROS scheme.

Chapter 12: An rf SQUID is inductively coupled to a tank circuit that connects to the readout electronics. According to the parameter β_e of rf SQUIDs, there are two working modes: the dissipative mode and the dispersive mode. In the dissipative mode, the rf SQUID acts as a damping resistance for the tank circuit; i.e. the quality factor of the tank circuit, Q, is changed with changing flux $\Delta\Phi$. In the dispersive mode, the rf SQUID is regarded as an additional inductance L_{SQ} inserted into the tank circuit, where the value of L_{SQ} is modulated with varying $\Delta\Phi$. However, for both working modes, the readout electronics is the same. The system noise $\delta\Phi_{sys}$ of the rf SQUID consists of three independent parts: the intrinsic SQUID noise $\delta\Phi_s$, the readout electronics noise $\delta\Phi_e$, and the thermal noise of the tank circuit, $\delta\Phi_T$, thus resulting in $\delta\Phi_{sys}^2 = \delta\Phi_s^2 + \delta\Phi_e^2 + \delta\Phi_T^2$. Conventionally, the pumping (resonance) frequency f_0 of the tank circuit is limited to approximately 30 MHz due to the distributed inductance and capacitance of the connection wires between the tank circuit at, e.g. 4.2 K, and the readout electronics at room temperature (RT). Taking an (capacitor-) inductor-tap on the tank circuit, the f_0 can rise up to the gigahertz range; thus the impedance across the tank circuit becomes very high. However, the impedance at the tap point remains low. Therefore, a standard 50 Ω transmission line is employed to connect the tap point of the tank circuit with the readout electronics at RT, where a bipolar transistor acts as a low-noise preamplifier. We define a dimensionless ratio κ to describe the position of the tap, where $\kappa = Z_{rf,input}/Z_{rf,T}$, in which the impedance $Z_{rf,input}$ at the tap point should approximately be 50 Ω and the high impedance $Z_{rf,T} = 2\pi f_0 L_T Q$ appears across the $L_T C_T$ tank circuit.

Two main achievements have been attained in HTS rf SQUID research: (i) Instead of the conventional $L_T C_T$ tank circuit, superconducting planar resonators or substrate resonators were developed for rf SQUID operation. This new kind of resonator possesses a high resonance frequency f_0 and a large quality factor Q_0, thus leading to a large $Z_{rf,T}$ across the tank circuit. To match the 50 Ω impedance, the ratio of $\kappa \ll 1$ can reduce the effective temperature of the tank circuit, thus decreasing its thermal noise, $\delta\Phi_T$. (ii) With such resonators, some high harmonic components of the $V_{rf}(\Phi)$ characteristics can be observed, thus changing the shapes of $V_{rf}(\Phi)$, where its slopes become steeper. Consequently, a large transfer coefficient ($\partial V_{rf}/\partial\Phi$) appears at the working point W, so the readout noise $\delta\Phi_e$ is suppressed. Ultimately, some HTS rf SQUIDs in resonator version demonstrated that their $\delta\Phi_{sys}$ was close to the SQUID's thermal noise limit. Furthermore, using a planar HTS field-to-flux transfer coil system with a pick-up area of $10 \times 10\,\mathrm{mm}^2$ in a three-layer structure, the HTS rf SQUID magnetometer

consisting of a thin-film rf SQUID and this transfer coil system in flip-chip configuration reached a field sensitivity of approximately 10 $fT/\sqrt{Hz}$ at 77 K.

References

1 Schwartz, B.B. and Foner, S. (1976). *Superconductor Applications: SQUIDs and Machines*. New York and London: Plenum Press.
2 Barone, A. and Paterno, G. (1982). *Physics and Applications of the Josephson Effect*. New York: Wiley.
3 Weinstock, H. (1996). *SQUID Sensors: Fundamentals, Fabrication and Applications*. Dordrecht: Kluwer Academic Publishers.
4 Clarke, J. and Braginski, A.I. (2004). *The SQUID Handbook*. Weinheim: Wiley-VCH.
5 Ryhänen, T., Seppä, H., Ilmoniemi, R., and Knuutila, J. (1989). SQUID magnetometers for low-frequency applications. *Journal of Low Temperature Physics* 76 (5–6): 287–386.
6 Simmonds, M.B. and Giffard, R.P. (1983). Apparatus for reducing low frequency noise in dc biased SQUIDs. US Patent 4, 389, 612.
7 Dutta, P. and Horn, P.M. (1981). Low-frequency fluctuations in solids – 1-F noise. *Reviews of Modern Physics* 53 (3): 497–516.
8 Weissman, M.B. (1988). 1/F noise and other slow, nonexponential kinetics in condensed matter. *Reviews of Modern Physics* 60 (2): 537–571.
9 Lam, S.K.H. (2006). Noise properties of SQUIDs made from nanobridges. *Superconductor Science & Technology* 19 (9): 963–967.
10 Cleuziou, J.P., Wernsdorfer, W., Bouchiat, V. et al. (2006). Carbon nanotube superconducting quantum interference device. *Nature Nanotechnology* 1 (1): 53–59.

2

Josephson Junctions

2.1 Josephson Equations

In 1962, Brian Josephson predicted a macroscopic quantum phenomenon, the Josephson effect [1], which became the basis of the superconducting quantum interference device (SQUID). A Josephson junction (JJ) is defined as two superconducting electrodes with weak coupling between them. One of the most widely adopted JJs is the superconductor–insulator–superconductor (SIS) tunnel contact, where the electrodes are separated by a thin insulating layer in thin-film techniques. The dc and ac properties of a JJ are described in the two Josephson equations (Eqs. (2.1) and (2.2)), thereby initiating the discipline of "superconducting electronics" [1, 2].

In the dc Josephson equation, a current I flowing through a JJ is given by

$$I = I_c \sin \delta \tag{2.1}$$

where δ is the phase difference in the macroscopic wave functions of the two superconducting electrodes. For each JJ, a critical current I_c exists. When $I < I_c$, the supercurrent I leads to a change in δ, while the voltage across the JJ remains zero ($U = 0$). Here, we assume that its current density is homogeneous in this junction area.

When $U \neq 0$ (e.g. $I > I_c$), the supercurrent I exhibits ac behavior, where the phase difference δ changes with time. The ac Josephson equation describes the relation between δ changes and the voltage U as follows:

$$\dot{\delta} = \frac{2e}{\hbar} U = \frac{2\pi}{\Phi_0} U \tag{2.2}$$

where e is the charge of an electron, $\hbar$ is Planck's constant, and $\Phi_0 \approx 2.07 \times 10^{-15}$ Wb is called the magnetic flux quantum.

2.2 RCSJ Model

Generally, an SIS-type tunnel junction can be described by the model of a resistively and capacitively shunted junction, the so-called RCSJ model. In this model, the Josephson element, represented by its critical current I_c, is connected in parallel with the junction capacitance C and a shunt resistance R_J

SQUID Readout Electronics and Magnetometric Systems for Practical Applications,
First Edition. Yi Zhang, Hui Dong, Hans-Joachim Krause, Guofeng Zhang, and Xiaoming Xie.

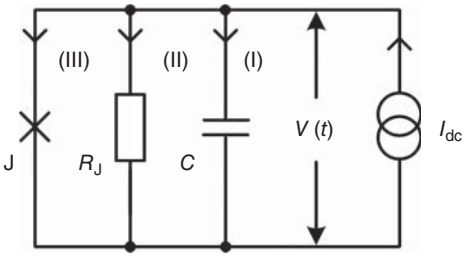

Figure 2.1 A Josephson element *J*, a capacitance *C*, and a resistance R_J are connected in parallel to form the RCSJ model.

as shown in Figure 2.1. When $I_{dc} > I_c$, an ac voltage across the parallel circuit appears, i.e. $V(t) \neq 0$. In this case, there are three different currents flowing through the junction: (I) $C[\mathrm{d}V(t)/\mathrm{d}t]$, the capacitive displacement current; (II) $V(t)/R$, the resistance current; and (III) $I_c \sin \delta(t)$, the ac supercurrent through the Josephson element [3, 4]. For instance, to understand the resistively and capacitively shunted junction (RCSJ) model, Sullivan and Zimmerman used the average angular velocity of a pendulum as a function of the applied torque to represent the analog of the current-to-voltage (I–V) characteristics of the junction, thus introducing damping concept into JJs [5]. The kinetic energy term of the pendulum can be the analog of the term $CV^2/2$, where C is the capacitance in branch (I) of Figure 2.1. Similarly, branches (II) and (III) have analogs in the pendulum system. To study the junction's features, one often employs its I–V characteristics, which are obtained by using a quasi-dc electrical measuring method. There, one frequently varies the current I_{dc} injected into the RCSJ junction while synchronously recording the voltage $V(t)$ across the junction, or vice versa. How one can obtain the I–V characteristics will be described in detail in Chapter 3. In fact, the I–V characteristics include information on the resistive and hysteretic behavior, although the rich physical meaning of the Josephson effects in Eqs. (2.1) and (2.2) cannot be fully reflected.

Usually, two parameters, β_c and Γ, are introduced to characterize the features of a JJ. In the RCSJ model, the Stewart-McCumber parameter β_c is denoted as

$$\beta_c = (2\pi/\Phi_0) I_c C R_J^2 \tag{2.3}$$

which describes the junction's hysteresis behavior, or, the damping classes. Figure 2.2 sketches the I–V characteristics of junctions for different β_c values. Generally, there are two extreme cases: (i) for $\beta_c \ll 1$, the junction is strongly damped with a small shunt resistance R_J. Consequently, the capacitive displacement current in Figure 2.1 does not play a role, so the I–V characteristics are single valued, i.e. nonhysteretic (see Figure 2.2a). In this case, the RCSJ model can be simplified to the so-called resistively shunted junction (RSJ) model [6]; (ii) when the resistance R_J is removed from the RCSJ model, the I–V characteristics become hysteretic, i.e. $\beta_c \to \infty$ (see Figure 2.2b) [7]. Here, the so-called capacitively shunted junction (CSJ) model is typically realized by an un-shunted tunnel contact with an SIS three-layer construction. In fact, $\beta_c = 1$ is the boundary between the nonhysteretic and hysteretic regimes in the junction's I–V characteristics. For $\beta_c = 2$, for example, hysteresis including a local loop clearly appears in the I–V characteristics (see Figure 2.2c).